Electrochemically Exfoliated Graphite/Cu/Cu$_2$O Composites and Their Photocatalytic Activity

Lia Destiarti[a], Oktaviardi Bityasmawan Abdillah[b], Retno Maharsi[b], Octia Floweri[c], Ferry Iskandar[b,c*]

[a]Department of Chemistry, Faculty of Mathematics and Natural Sciences, Universitas Tanjungpura, Jl. Prof. Dr. Hadari Nawawi, Pontianak, 78114, Indonesia
[b]Department of Physics, Faculty of Mathematics and Natural Sciences, Institut Teknologi Bandung, Jl. Ganesha 10, Bandung, 40132, Indonesia
[c]Research Center for Nanosciences and Nanotechnology, Institut Teknologi Bandung, Jl. Ganesha 10, Bandung 40132, Indonesia

*Email: ferry@fi.itb.ac.id

Abstract

In this work, the photocatalytic performance of electrochemically exfoliated graphite (EG) with low copper addition (≤ 5 wt.%) was studied. Composites of EG/Cu/Cu$_2$O were successfully prepared by microwave-assisted in situ reduction method. FTIR spectra of the samples showed that the main functional groups of graphite were detected in the samples. XRD characterization further proved the presence of EG, Cu, and Cu$_2$O in the samples. The higher proportion of Cu$_2$O presented in the samples prepared with a higher amount of Cu^{2+}. SEM analysis showed that Cu$_2$O/Cu particles were homogeneously deposited on the surface of EG. The composites of EG, Cu, and Cu$_2$O with a varied amount of Cu (1 and 5 wt. %) in EG / Cu^{2+} mixture were examined as photocatalyst in the degradation process of Rhodamine B (RhB). The photocatalytic degradation of RhB was analysed by observing its decolorization within a set time of irradiation. UV-Vis analysis revealed that the degradation of RhB in EG/Cu/Cu$_2$O A and B for 105 minutes was 26 and 35 %, respectively. The result demonstrates that the sample with a larger amount of Cu$_2$O (sample B, Cu 5 wt.%) shows higher photocatalytic activity in the degradation of RhB.

Keywords: photocatalysts, exfoliated graphite/copper composite, rhodamine B

1. Background

Exfoliated graphite (EG) refers to graphite with a degree of separation of a substantial portion of the carbon layers in the graphite [1]. This material has been gaining tremendous attention due to its excellent properties, including large surface area, high porosity, and high charge carrier mobility [2]. These properties make EG suitable for the application as catalyst support, gaskets, and anode of lithium battery [1,3,4]. EG is also easy to fabricate using several top-down processes from graphite precursor, such as chemical exfoliation [5], thermal exfoliation [6], and electrochemical exfoliation [7]. Among them, the electrochemical exfoliation technique is considered more accessible, environmentally friendly, economically profitable, and applicable to mass production [7,8].

Our previous research has demonstrated the efficient graphite exfoliation via the electrochemical process with the aid of H$_2$SO$_4$/H$_2$O$_2$ pretreatment [9]. This method can cut down the processing time that is typically needed to exfoliate graphite using other complex processes. Moreover, unlike the chemical exfoliation method, which involves the reduction process to transform an oxidized form of EG or Exfoliated Graphite Oxide (EGO) to its reduced form (rEGO), this method does not need the reduction process to produce EG [5].

To this day, the research of EG has been evolving dynamically. Functionalization and deposition of EG have been involved in improving its properties to be applied in various applications [10,11]. Among materials that have been studied, metals [12] and metal oxides [10,13] have been frequently deposited on the EG surface.

There are several ways to deposit metals and metal oxides on the surface of EG, such as in situ chemical reduction [10,14], solvothermal/hydrothermal [15], and electrodeposition [16]. Among them, the in situ reduction process has been utilized to deposit metal on several types of carbonaceous, such as EG [17], rGO [14], and CNT [18]. In our previous work, we intended to deposit Cu on the GO surface through the microwave-assisted reduction of Cu^{2+} ions to produce rGO/Cu composites [14]. However, it was revealed that depends on the added amount of copper precursor, Cu species

presented in various forms, i.e., Cu, Cu_2O, and CuO. It was also demonstrated that the species of Cu, determined the electrical conductivity of the resulted rGO composites. Samples prepared with a higher content of copper oxides (Cu_2O and CuO) showed lower electrical conductivity due to the semiconducting/insulating properties of copper oxide. Whereas, the sample with a higher content of metallic Cu showed higher electrical conductivity due to the nature of metallic Cu.

Despite its low electric conductivity, copper (I) oxide (Cu_2O), along with other semiconducting metal oxides such as TiO_2 [19], ZnO [20], and SnO_2 [21], are known to have the ability to perform the photocatalytic reaction. These materials can absorb light to excite electrons from the valence band (VB) to conduction band (CB) and leave holes in the VB [22]. The generated electron-hole pairs move to the surface of the material to perform a redox reaction with the organic compounds. However, this process is commonly hampered by the fast recombination of electron-hole pairs, reducing photocatalytic efficiency.

Many researchers have attempted to composite photocatalyst materials with support materials, commonly carbonaceous materials, to improve photocatalytic efficiency. Among the carbonaceous material, EG is one of candidates as photocatalyst support material due to its exceptional properties, including high charge carrier conductivity and large surface area, which are beneficial for photocatalytic application. High charge carrier conductivity is responsible for preventing fast recombination of electron-hole pairs [3,23]. Meanwhile, a large surface area is beneficial to provide more active sites for photocatalytic reaction [2,24]. In addition to EG, Cu metals could also improve the transport of photoelectrons, which leads to efficient charge (electron-hole) separation [25,26]. Therefore, the enhancement of photocatalytic performance is expected to be achieved by compositing EG, Cu, and Cu_2O.

Previously, our group has studied the effect of compositing rGO with a small amount of copper ($\leq$ 5 wt.%), from which we have obtained rGO, Cu, and Cu_2O composite. However, despite the expected excellent performance, there has been no report about its photocatalytic performance. In this study, EG which resembles the characteristics of rGO was mixed with Cu^{2+} ions. The mixture then underwent a reduction procedure under microwave irradiation with hydrazine as a reducing agent, following a similar procedure in our previous work [14]. EG was prepared using the electrochemical exfoliation method which is more efficient than the modified Marcano method that was studied in our previous research. The action is expected to produce a composite of EG/Cu/Cu_2O due to the incomplete reduction of Cu^{2+} ions. The obtained EG/Cu/Cu_2O composites were characterized using XRD, FT-IR, and SEM to assess the effect of Cu/Cu_2O addition on the exfoliation, functionalization, and morphology of EG, respectively. Hereinafter, the photocatalytic activity of the obtained EG/Cu/Cu_2O composite was evaluated through the decolorization process of rhodamine B (RhB).

2. Methodology

2.A. Preparation of Exfoliated Graphite/Copper (EG/Cu/Cu_2O) Composites

In this study, EG was produced via electrochemical exfoliation of graphite following the procedure demonstrated in our previous work [9]. The graphite precursor was immersed in a mixed solution of H_2SO_4 98% with H_2O_2 50%, with the ratio of H_2SO_4 to H_2O_2 was 95:5. After 5 minutes of immersion, the graphite precursor was then exfoliated employing an anodic electrochemical process. This process was conducted at the potential of 15 V, inside a beaker glass containing 0.1 M aqueous solution of $(NH_4)_2SO_4$ as an electrolyte. The obtained sample was rinsed using DI water and ethanol. After washing, the sample was then dried in the oven at 60 ^{o}C for 2h. This sample is labeled as raw EG.

EG/Cu/Cu_2O composites were fabricated by firstly preparing EG suspensions by mixing raw EG in ethylene glycol (Merck, 1 ml for 1 mg EG). The mixture was sonicated for 30 minutes and then vacuum filtrated to separate its residue and supernatant. After that, a certain amount of $Cu(NO_3)_2 \cdot 2H_2O$ (Merck) was added to the supernatant to obtain EG/Cu^{2+} dispersion with Cu composition of 1 and 5 wt. %. The dispersion was stirred for 15 minutes and followed by sonication and homogenization process using Ultra-Turrax homogenizer for 40 minutes. The reduction process was conducted by adding hydrazine (Merck, 1 ml for 1 g of EG), followed by stirring for 15 min and low mode microwave treatment (Panasonic Microwave 2.45 MHz, 800 W) for 20 min. The obtained sample was rinsed using DI water and

ethanol and followed by drying in an oven at 80°C for 2h. The obtained samples were labeled as EG, EG/Cu/Cu$_2$O A, and EG/Cu/Cu$_2$O B for 0 wt.%, 1 wt.%, and 5 wt.% Cu [in the form of Cu(NO$_3$)$_2$.2H$_2$O] added to the EG, respectively.

2.B. Characterization of EG/Cu Composites

The obtained EG/Cu/Cu$_2$O composites were characterized using Fourier Transform Infra-Red (FTIR) Spectrometer Prestige 21 Shimadzu and Bruker D8 Advance X-Ray Diffractometer (XRD) with Cu-Kα radiation (λ=1,54056 Å) to analyze the functional group and the structure of the composites. Meanwhile, the morphology of the samples was observed using a Scanning Electron Microscope - SEM Hitachi SU3500.

2.C. Photocatalytic Activity Measurement

The photocatalytic activity of the EG/Cu/Cu$_2$O composite was evaluated by observing the degradation process of RhB. For this measurement, 0.02 g of EG/Cu/Cu$_2$O composite was mixed with 50 mL of RhB aqueous solution (2 mg/L). In the dark, the mixtures were then irradiated by three UV blacklight lamps with a power of 10 W. Afterward, 3 mL of each mixture was drawn at regular intervals of 15, 45, 75, and 105 min, then membrane filtrated to remove the catalyst. The supernatant was then measured using Micro pack UV-Vis-NIR light DH-2000-BAL at the range of 400-750 nm. The concentration of RhB in each supernatant was determined using the following Lambert – Beer equation

$$A = abC ,\qquad (1)$$

where A, a, b, and C are absorbance, molar attenuation coefficient, optical path length, and solution concentration, respectively. The calibration curve which showed a linear response (r^2=0.9906) was obtained by measuring the absorbance of a series RhB standard solution (0.50-3.00 mg/L) at λ_{max} of 554 nm.

3. Results and Discussion

Figure 1 shows FTIR spectra of the raw EG and EG/Cu/Cu$_2$O composites. All spectra show several dominant peaks which are commonly present in graphitic materials such as peaks at 2930 cm^{-1}, 1080 cm^{-1}, and 1500-1650 cm^{-1}, each corresponds to stretching of C-H, stretching of C-O, and asymmetric stretching vibration of C=C, respectively. At the range of C=C vibration characteristic, there are two peaks that are located
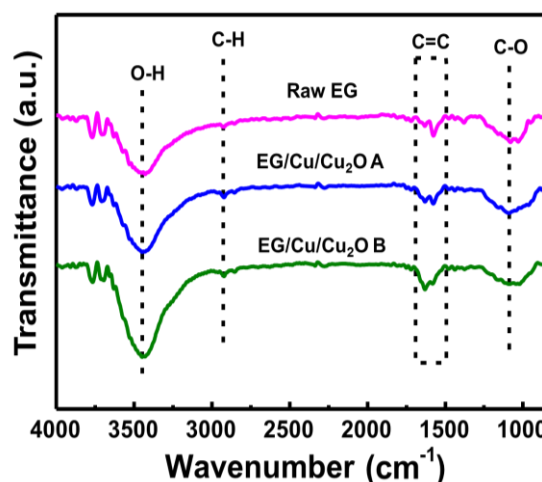
Figure 1. FTIR spectra of raw EG, EG/Cu/Cu$_2$O A, and EG/Cu/Cu$_2$O B.

at ca. 1580 cm^{-1} and 1630 cm^{-1}. The C=C peak at 1580 cm^{-1} is known to correspond to the vibrational mode of substituted aromatic rings in graphitic material, which corresponds to the introduction of oxygen-containing functional group in graphitic material [27]. Meanwhile, the C=C peak at 1630 cm^{-1} corresponds to the unoxidized sp^2 graphitic network [28].

Figure 1 shows that the intensity of C=C peak at 1580 cm^{-1} tends to decrease with respect to C=C peak at 1630 cm^{-1} with the increasing amount of Cu loading. This result indicates that the higher Cu amount leads to a lower oxygen-containing functional group in EG. The broad and strong peak related to the vibration of the hydroxyl (-OH) group also can be seen from all samples at a wavenumber of 3000-3700 cm^{-1}. However, the width of -OH peak tends to be narrower with the more addition of Cu to EG. The narrowing of -OH peak is related to lower content of hydroxyl group in the sample EG/Cu/Cu$_2$O B than other samples [29,30]. This phenomenon is allegedly caused by the ability of Cu^{2+} to work as a reducing agent in the reduction of oxygenated carbonaceous compounds under microwave irradiation. A similar result has been reported by Li et al. in the process of graphene oxide reduction by metallic Cu [31].

Figure 2 (a) shows the x-ray diffractograms of raw graphite, EG, EG/Cu/Cu$_2$O A, and EG/Cu/Cu$_2$O B. A peak at 2θ of 26.3°, which corresponds to (002) plane of graphitic structure (JCPDS-41-1487), can be seen from all samples. However, the intensity of the peak significantly decreased in the EG, EG/Cu/Cu$_2$O A, and EG/Cu/Cu$_2$O B samples compared to the raw graphite sample, indicating
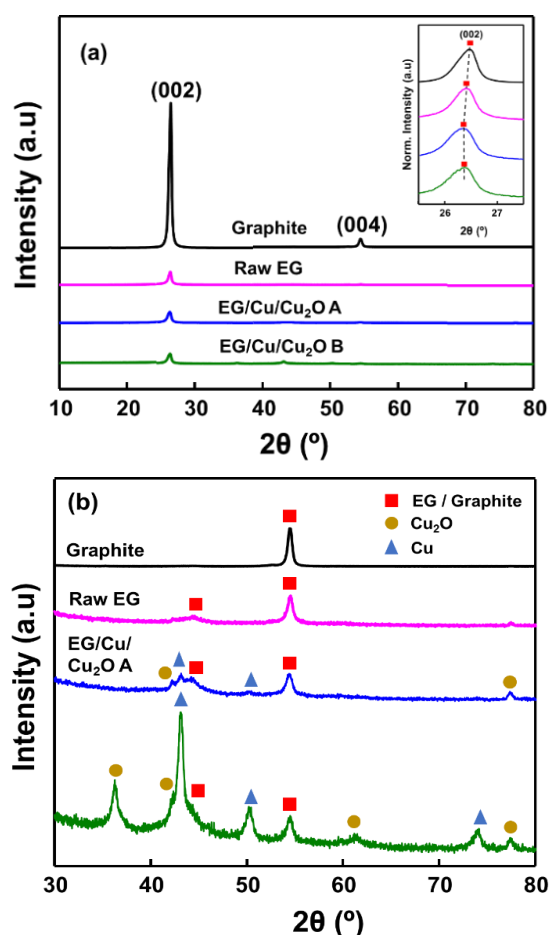
Figure 2. XRD patterns of graphite, raw EG, EG/Cu/Cu$_2$O A, and EG/Cu/Cu$_2$O B at (a) 2θ of 10°-80° and (b) 2θ of 30°-80°. The inset graph (a) shows the enlargement of diffraction patterns along 2θ of 25.5-27.5 °.

the disruption of graphene layer stacking along c-axis in these samples. This result implies that graphite was exfoliated into fewer layers as reported by several studies [32–34].

Inset Figure 2(a) shows the intensity normalized diffractograms of all samples. It can be seen that the (002) peak was shifted from 2θ of 26.46° (graphite sheet) to 26.40° (EG), which also confirmed the exfoliation of graphite [33,34]. The calculation result of (002) plane interlayer spacing (d$_{002}$) using Bragg Equation, shown in table 1, revealed that interlayer spacing of (002) plane increased from 3.364 (raw graphite) to 3.371 Å (EG).

The addition of Cu to EG also affected the interlayer spacing of (002) plane of EG. The interlayer spacing of EG increased to 3.379 and 3.382 Å in the samples prepared with the addition of 1 and 5 wt. % of Cu, respectively. The increasing of interlayer spacing in EG sample with Cu addition

might be attributed to partial insertion of Cu or Cu$_2$O particle between interlayer of graphite layers [35]. As the increasing amount of Cu addition, more particles were inserted into graphite interlayer which caused the larger interlayer spacing of EG/Cu/Cu$_2$O B than EG/Cu/Cu$_2$O A. Not only had it caused the increase of interlayer spacing of (002) plane, exfoliation of graphite, and addition of Cu also caused the decrease of crystallite size of the graphitic plane. It can be seen from Table 1 that the crystallite size of (002) plane decreased from 184.19 (graphite sheet) to as low as 127.59 Å (EG/Cu 5 wt. %).

Figure 2 (b) exhibits the diffractograms of graphite, raw EG, EG/Cu/Cu$_2$O A, and EG/Cu/Cu$_2$O B at range 2θ of 30°-80°. In this figure, there are several peaks represent EG, Cu, and Cu$_2$O in the sample which is not visible in Figure 2 (a) due to the dominant intensity of (002) graphitic peak. The peak at 2θ of 44.5° and 55.0° correspond to (101) and (004) plane of EG, respectively. The peaks at 2θ of 44° and 52° correspond to (111) and (200) planes of Cu (JCPDS-04-0836). Meanwhile, peaks that appeared at 2θ of 36°, 42.5°, 61.5°, 74°, and 78° correspond to (111), (200), (220), (311), and (222) planes of Cu$_2$O, respectively (JCPDS-05-0667). Upon the addition of hydrazine, the reduction process of Cu^{2+} caused the formation of Cu and Cu$_2$O. Cu$_2$O was formed due to incomplete reduction of Cu^{2+} which possibly caused by the lack amount of hydrazine.

Another mechanism of Cu$_2$O formation was probably due to reduction reaction of oxygen functional group in EG by nascent metallic Cu. As indicated by XRD and FTIR characterization, the reduction of EG by Cu may cause the re-oxidation of the Cu. Higher peak intensities of Cu and Cu$_2$O can be seen clearly from the EG sample prepared by the addition of 5 wt. % of Cu, noting the higher amount of Cu^{2+} added. It also can be seen that the Cu$_2$O phase is more dominant than the Cu phase in this sample, as peaks correspond to Cu$_2$O were more to be found.

Quantitative analysis comparing the peak area of Cu$_2$O to peak area of Cu (Table 1) in both samples prepared with the addition of Cu^{2+} also showed the same trend. The sample prepared by adding 5 wt. % of Cu^{2+} showed a higher ratio of Cu$_2$O to Cu compared to that of prepared with 1 wt. % of Cu^{2+}. This phenomenon allegedly happened because the amount of hydrazine involved in the reduction was

Table 1. Comparison of d_{hkl} and L of synthesized materials.

Sample	2θ (deg)	FWHM (deg)	d_{002} (Å)	L (Å)	Cu_2O/Cu peaks area
Graphite	26.46	0.46	3.364	184.19	-
Raw EG	26.40	0.53	3.372	159.84	-
EG/Cu/Cu_2O A	26.34	0.66	3.379	128.88	0.63
EG/Cu/Cu_2O B	26.32	0.67	3.382	127.59	1.51

d_{002} = interplanar spacing (derived from Bragg Law)
FWHM = full width at half maximum of a diffraction peak
L = average crystallite size (derived from Debye-Scherrer equation)

not enough to ultimately reduce Cu^{2+} to Cu (s) in this sample.

SEM characterization was conducted to study the effect of the addition of different copper concentration on the morphology of EG/Cu/Cu_2O composites. The SEM images of EG/Cu/Cu_2O A and EG/Cu/Cu_2O B are shown in Figure 3 (a) and (b), respectively. As can be seen from the images, small particles were deposited on the surface of both samples. Indeed, more particles can be observed on the surface of the sample with a higher copper content (EG/Cu 5 wt. %). This result corresponds to XRD analysis that demonstrated a higher intensity of Cu and Cu_2O peaks in the sample prepared with a larger amount of copper addition. Larger copper addition also caused the Cu and Cu_2O particles evenly decorated the surface EG than that of samples with the smaller copper amount. The larger amount and more evenly distribution of Cu/Cu_2O particles are expected to provide larger active sites for enhancing photocatalytic performance.

The photocatalytic activities of EG/Cu/Cu_2O A and EG/Cu/Cu_2O B composites were principally evaluated by degradation of hazardous of RhB, a kind of cationic dyes which gives pinkish-red color when dissolved in water. Absorbance spectra of RhB aqueous solution measured using a UV-Vis spectrophotometer at 400-700 nm are shown in figure 4. Figure 4 (a) and (b) show absorbance spectra oh RhB solution with the addition of

EG/Cu/Cu_2O A and EG/Cu/Cu_2O B, respectively. The spectra were taken after irradiation of RhB solution for particular irradiation time (0, 15, 45, 75, and 105 mins). It can be seen from both cases that absorbance peaks at λ_{max} of 554 nm decreased with increasing irradiation time. However, the EG/Cu/Cu_2O B generally showed higher activity than the EG/Cu/Cu_2O A.

The photocatalytic activities of EG/Cu/Cu_2O composites on the degradation process of RhB were also demonstrated via the plot of degradation efficiency (h(%)) as a function of time (min). The degradation efficiency (h%) was calculated using the formula of $h(\%) = (1 - C/C_0) \times 100\%$, where C is the concentration of the RhB at a reaction time of t min and C_0 is the concentration of RhB at a reaction time of 0 min [36].

The data in Figure 4.c demonstrated that samples prepared with 5 wt. % of Cu showed an efficiency value of 35 %, higher than that of
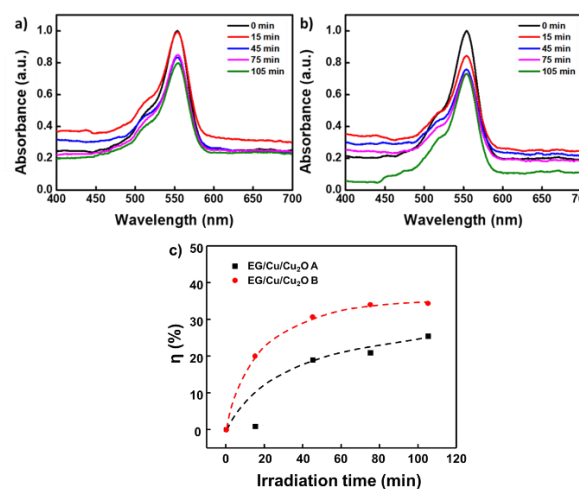
Figure 4. The UV-Vis spectra of RhB aqueous solution measured with increasing irradiation time (a) with EG/Cu/Cu_2O A and (b) EG/Cu/Cu_2O B as the photocatalyst. (c) The photocatalytic degradation efficiency versus irradiation time with EG/Cu/Cu_2O A and EG/Cu/Cu_2O B as the photocatalyst.

Figure 3. SEM images of (a) EG/Cu/Cu_2O A and (b) EG/Cu/Cu_2O B.

prepared with a smaller amount of Cu (1 wt. %) with an efficiency value of 26 % during 105 min of irradiation. This phenomenon probably happened due to the higher amount of Cu_2O compound presented in the sample with 5 wt. % of Cu.

As explained previously, Cu_2O may act as a photocatalyst that increases the photodegradation rate of RhB. Han et al. [37] reported the significance of Cu_2O in the photocatalytic activity of Cu_2O/TiO_2 composite. Photocatalyst with a higher content of Cu_2O showed higher photocatalytic activity in degrading the dye pollutant [37]. Zhao et al. have also reported that compositing Cu_2O with rGO could improve the photocatalytic activity of the catalyst to degrade methylene orange [24]. The narrow bandgap of Cu_2O (~ 2 eV) allows the absorption of the photon at the visible region to excite an electron from the conductance band to the valence band in Cu_2O [38]. During this process, a pair of electron-hole is generated, and each may indirectly reduce or oxidize organic dyes. The electrons that are flowing through EG reacts with an O_2 molecule generating an unstable $\cdot O_2^-$ molecule. Meanwhile, the photogenerated holes (h^+) with strong oxidation ability could interact with H_2O to produce radical hydroxyl ($\cdot OH$) [39]. The generated species ($\cdot O_2^-$, $\cdot OH$) can degrade the RhB and other organic dyes [24,37].

4. Conclusion

In this study, $EG/Cu/Cu_2O$ composite was successfully prepared. The addition of hydrazine to EG/Cu salt mixture caused the reduction of Cu^{2+} to form Cu and Cu_2O, as confirmed by XRD. The more significant proportion of Cu_2O was observed from the sample prepared with a higher amount of Cu^{2+} ($EG/Cu/Cu_2O$ B). This occurrence allegedly happened due to incomplete reduction of Cu^{2+} affected by the lack of a reducing agent (hydrazine). It was demonstrated that samples with a larger amount of Cu_2O showed higher photocatalytic activity in the degradation of RhB with optimum efficiency of 35% after 105 min of irradiation.

5. Acknowledgements

References

[1] Chung, D. D. L., A review of exfoliated graphite, Journal of Materials Science, 51(1), pp.554–568, 2016.

[2] Malefane, M. E., Feleni, U., and Kuvarega, A. T., A tetraphenylporphyrin /WO₃ /exfoliated graphite nanocomposite for the photocatalytic degradation of an acid dye under visible light irradiation, New Journal of Chemistry, 43(28), pp.11348–11362, 2019.

[3] Singh, P., Shandilya, P., Raizada, P., Sudhaik, A., Rahmani-Sani, A., and Hosseini-Bandegharaei, A., Review on various strategies for enhancing photocatalytic activity of graphene based nanocomposites for water purification, Arabian Journal of Chemistry, 13(1), pp.3498–3520, 2020.

[4] Agostini, M. , Brutti, S. , and Hassoun, J., High Voltage Li-Ion Battery Using Exfoliated Graphite/Graphene Nanosheets Anode, ACS Applied Materials & Interfaces, 8(17), pp.10850–10857, 2016.

[5] Stankovich, S., Dikin, D. A., Piner, R. D., Kohlhaas, K. A., Kleinhammes, A., Jia, Y., Wu, Y., Nguyen, S. T., and Ruoff, R. S., Synthesis of graphene-based nanosheets via chemical reduction of exfoliated graphite oxide, Carbon, 45(7), pp.1558–1565, 2007.

[6] Poh, H. L., Simek, P., Sofer, Z., and Pumera, M., Sulfur-doped graphene via thermal exfoliation of graphite oxide in H₂S, SO₂, or CS₂ gas, ACS nano, 7(6), pp.5262–5272, 2013.

[7] Yu, P., Lowe, S. E., Simon, G. P., and Zhong, Y. L., Electrochemical exfoliation of graphite and production of functional graphene, Current opinion in colloid & interface science, 20(5–6), pp.329–338, 2015.

[8] Abdelkader, A. M., Patten, H. V., Li, Z., Chen, Y., and Kinloch, I. A., Electrochemical exfoliation of graphite in quaternary ammonium-based deep eutectic solvents: a route for the mass production of graphane, Nanoscale, 7(26), pp.11386–11392, 2015.

[9] Iskandar, F., Abdillah, O.B., Mayangsari, T.R. and Aimon, A.H., Preliminary Study of Graphite Rod Pre-treatment in H₂O₂/H₂SO₄ Mixture Solution on the Synthesized Graphene by Electrochemical Exfoliation Method, in 2018 5th International Conference on Electric Vehicular Technology (ICEVT), pp. 46-48, 2019.

[10] Zhang, M., Lei, D., Du, Z., Yin, X. , Chen, L., Li, Q., Wang, Y., and Wang, T., Fast synthesis of SnO₂/graphene composites by reducing graphene oxide with stannous ions, Journal of Materials Chemistry, 21(6), pp.1673–1676, 2011.

[11] Kuila, T., Bose, S., Mishra, A. K., Khanra, P., Kim, N. H., and Lee, J. H., Chemical functionalization of graphene and its applications, Progress in Materials Science, 57(7), pp.1061–1105, 2012.

[12] Lu, J., Do, I., Drzal, L. T., Worden, R. M., and Lee, I., Nanometal-decorated exfoliated graphite nanoplatelet based glucose biosensors with high sensitivity and fast response, ACS nano, 2(9), pp.1825–1832, 2008.

[13] Xu, C., Wang, X., Zhu, J., Yang, X., and Lu, L., Deposition of Co_3O_4 nanoparticles onto exfoliated graphite oxide sheets, Journal of Materials Chemistry, 18(46), pp.5625–5629, 2008.

[14] Iskandar, F., Abdillah, O. B., Stavila, E., and Aimon, A. H., The influence of copper addition on the electrical conductivity and charge transfer resistance of reduced graphene oxide (rGO), New Journal of Chemistry, 42(19), pp.16362–16371, 2018.

[15] Zhang, L. Y., Zhao, Z. L., Yuan, W., and Li, C. M., Facile one-pot surfactant-free synthesis of uniform Pd_6Co nanocrystals on 3D graphene as an efficient electrocatalyst toward formic acid oxidation, Nanoscale, 8(4), pp.1905–1909, 2016.

[16] Yang, L., Yan, D., Liu, C., Song, H., Tang, Y., Luo, S., and Liu, M., Vertically oriented reduced graphene oxide supported dealloyed palladium–copper nanoparticles for methanol electrooxidation, Journal of Power Sources, 278pp.725–732, 2015.

[17] Zhang, H., Jin, Z., Han, L., and Qin, C., Synthesis of nanoscale zero-valent iron supported on exfoliated graphite for removal of nitrate, Transactions of Nonferrous Metals Society of China, 16, pp.s345–s349, 2006.

[18] Alimohammadi, F., Gashti, M. P., Shamei, A., and Kiumarsi, A., Deposition of silver nanoparticles on carbon nanotube by chemical reduction method: Evaluation of surface, thermal and optical properties, Superlattices and Microstructures, 52(1), pp.50–62, 2012.

[19] Tachikawa, T., Fujitsuka, M., and Majima, T., Mechanistic insight into the TiO2 photocatalytic reactions: design of new photocatalysts, The Journal of Physical Chemistry C, 111(14), pp.5259–5275, 2007.

[20] Behnajady, M. A., Modirshahla, N., and Hamzavi, R., Kinetic study on photocatalytic degradation of CI Acid Yellow 23 by ZnO photocatalyst, Journal of hazardous materials, 133(1–3), pp.226–232, 2006.

[21] Cun, W., Jincai, Z., Xinming, W., Bixian, M., Guoying, S., Ping'an, P., and Jiamo, F., Preparation, characterization and photocatalytic activity of nano-sized ZnO/SnO2 coupled photocatalysts, Applied Catalysis B: Environmental, 39(3), pp.269–279, 2002.

[22] Schneider, J., Matsuoka, M., Takeuchi, M., Zhang, J., Horiuchi, Y., Anpo, M., and Bahnemann, D. W., Understanding TiO_2 Photocatalysis: Mechanisms and Materials, Chemical Reviews, 114(19), pp.9919–9986, 2014.

[23] Baldissarelli, V. Z., Souza, T. de, Andrade, L., Oliveira, L. F. C. de, José, H. J., and Moreira, R. de F. P. M., Preparation and photocatalytic activity of TiO_2-exfoliated graphite oxide composite using an ecofriendly graphite oxidation method, Applied Surface Science, 359, pp.868–874, 2015.

[24] Zhao, Q., Wang, J., Li, Z., Qiao, Y., Jin, C., and Guo, Y., Preparation of Cu_2O/exfoliated graphite composites with high visible light photocatalytic performance and stability, Ceramics International, 42(11), pp.13273–13277, 2016.

[25] Wang, H., Hu, Y., Jiang, Y., Qiu, L., Wu, H., Guo, B., Shen, Y., Wang, Y., Zhu, L., and Xie, A., Facile synthesis and excellent recyclable photocatalytic activity of pine cone-like $Fe_3O_4@Cu_2O$/Cu porous nanocomposites, Dalton Transactions, 42(14), pp.4915–4921, 2013.

[26] Wang, P., Qi, C., Hao, L., Wen, P., and Xu, X., Sepiolite/Cu_2O/Cu photocatalyst: Preparation and high performance for degradation of organic dye, Journal of Materials Science & Technology, 35(3), pp.285–291, 2019.

[27] Kumar, N. and Srivastava, V. C., Simple Synthesis of Large Graphene Oxide Sheets via Electrochemical Method Coupled with Oxidation Process, ACS Omega, 3(8), pp.10233–10242, 2018.

[28] Țucureanu, V., Matei, A., and Avram, A. M., FTIR Spectroscopy for Carbon Family Study, Critical Reviews in Analytical Chemistry, 46(6), pp.502–520, 2016.

[29] Li, W. and Yang, Y. J., The reduction of graphene oxide by elemental copper and its application in the fabrication of graphene supercapacitor, Journal of Solid State Electrochemistry, 18(6), pp.1621–1626, 2014.

[30] Zhou, M., Tang, J., Cheng, Q., Xu, G., Cui, P., and Qin, L.-C., Few-layer graphene obtained by electrochemical exfoliation of graphite cathode, Chemical Physics Letters, 572, pp.61–65, 2013.

[31] Wang, H., Wei, C., Zhu, K., Zhang, Y., Gong, C., Guo, J., Zhang, J., Yu, L., and Zhang, J., Preparation of Graphene Sheets by Electrochemical Exfoliation of Graphite in

Confined Space and Their Application in Transparent Conductive Films, ACS Applied Materials & Interfaces, 9(39), pp.34456–34466, 2017.

[32] Geng, X., Guo, Y., Li, D., Li, W., Zhu, C., Wei, X., Chen, M., Gao, S., Qiu, S., Gong, Y., Wu, L., Long, M. , Sun, M. , Pan, G. , and Liu, L. , Interlayer catalytic exfoliation realizing scalable production of large-size pristine few-layer graphene, Scientific Reports, 3(1), pp.1134, 2013.

[33] Zhou, M., Tang, J., Cheng, Q., Xu, G., Cui, P., and Qin, L. C., Few-layer graphene obtained by electrochemical exfoliation of graphite cathode, Chemical Physics Letters, 572, pp.61–65, 2013.

[34] Wu, L., Li, W., Li, P., Liao, S., Qiu, S., Chen, M., Guo, Y., Li, Q., Zhu, C., and Liu, L., Powder, Paper and Foam of Few-Layer Graphene Prepared in High Yield by Electrochemical Intercalation Exfoliation of Expanded Graphite, Small, 10(7), pp.1421–1429, 2014.

[35] Han, L., Liu, C.-M., Dong, S.-L., Du, C.-X., Zhang, X.-Y., Li, L.-H., and Wei, Y., Enhanced conductivity of rGO/Ag NPs composites for electrochemical immunoassay of prostate-specific antigen, Biosensors and Bioelectronics, 87, pp.466–472, 2017.

[36] Nguyen, D. C. T., Cho, K. Y., and Oh, W.-C., Synthesis of mesoporous SiO_2/Cu_2O–graphene nanocomposites and their highly efficient photocatalytic performance for dye pollutants, RSC Advances, 7(47), pp.29284–29294, 2017.

[37] Han, T., Zhou, D., Wang, H., and Zheng, X., The study on preparation and photocatalytic activities of Cu_2O/TiO_2 nanoparticles, Journal of Environmental Chemical Engineering, 3(4, Part A), pp.2453–2462, 2015.

[38] Wang, Y. , Lany, S., Ghanbaja, J., Fagot-Revurat, Y., Chen, Y. P., Soldera, F., Horwat, D., Mücklich, F., and Pierson, J. F., Electronic structures of Cu_2O, Cu_4O_3, and CuO: A joint experimental and theoretical study, Physical Review B, 94(24), pp.245418, 2016.

[39] Xiaolin, D. , Zi, W., Jinjing, P., Wenli, G., Qiao, L., Lin, L., and Juming, Y., High photocatalytic activity of $Cu@Cu_2O/RGO$/cellulose hybrid aerogels as reusable catalysts with enhanced mass and electron transfer, Reactive and Functional Polymers, 138, pp.79–87, 2019.